www.amlett.com, www.amlett.org, DOI: 10.5185/amlett.2013.2429 Published online by the VBRI press in 2013

Morphological and impedance studies in diluted Mn-doped CdS nanocomposites

P. Venkatesu[1*], K. Ravichandran[2], B. K. Reddy[3]

[1]*Department of Physics, N. B. K .R Institutes, Vidyanagar 524413, India*
[2]*Department of Nuclear Physics, University of Madras, Chennai 600025, India*
[3]*Department of Physics, Sri Venkateswara University, Tirupathi 517502, India*

[*]Corresponding author. Tel: (+91) 9912868469; E-mail: venkateshpudi@yahoo.co.in

Received: 28 February 2013, Revised: 20 April 2013 and Accepted: 01 May 2013

ABSTRACT

Nanocrystalline samples of Cadmium Sulphide (CdS) were prepared with different Manganese (Mn) doping concentrations (0-10 at.%) through chemical route using thiophenol as a capping agent. Fourier Tranform Infrared Spectroscopy (FT-IR) study disclosed the presence of capping agent on the surface of the samples. X-ray diffraction (XRD) analysis showed phase transition from hexagonal to cubic phase beyond 8 at.% of Mn doping and grain size in the range of 13-30 nm. Micro structural study by High Resolution Transmission Electron Microscopy (HRTEM) confirmed phase transition and quasi-spherical particles having size in 15-50 nm range with small grains distributed on the surface of the particles. A blue shift in the band gap energy of the samples was indicated in optical absorption study and the band gap was found to vary nonlinearly with Mn content. Studies on electrical properties of the samples using a complex impedance spectroscopy (CIS) technique showed a decrease in the bulk resistance with increase in Mn concentration. Further, the nature of cole-cole plots (Nyquist plots) revealed the presence of bulk and grain boundary effects in the samples in consistent with HRTEM results. These crystalline quasi-spherical nanoparticles of CdS:Mn seems to be one of the promising candidates for modern age opto-electronics and biomedical applications. Copyright © 2013 VBRI press.

Keywords: CdS: Mn; phase transition; blue shift; cole-cole plots.

P. Venkatesu is currently working as a lecturer in the department of Physics, N.B.K.R Institutes, Vidyanagar-524413, India. He obtained his graduate degree in Physics from Sri Venkateswara Arts College, Tirupathi, and M. Sc. From Sri Venkateswara University, Tirupathi in the year 1997. He did his Ph. D. in Physics in Diluted Magnetic Semi-conducting nanomaterials at Sri Venkateswara University, Tirupathi in the year 2008. His research interests are Synthesis of Nanocrystalline Magnetic materials.

K. Ravichandran is a faculty in the Department of Nuclear Physics, University of Madras, Chennai-600025 India. He obtained his graduate degree in Physics from Madras University. M.Sc. and M. Phil from University of Madras and Anna University, respectively. He obtained his Ph. D. in Physics with Scientific Instrumentation from University of Madras Chennai. His research interests are Synthesis of Nanocrystalline Magnetic materials, Metallic oxide materials, Spintronics and Nano-ferrofluids for drug delivery systems.

Introduction

Diluted magnetic semiconductors (DMS) have been studied widely during the past two decades in view of their intriguing properties [**1-2**]. On the other hand, consequent upon the advent of nanomaterials, DMS in nano-form have in recent years attracted significant attention of the technologists, because of their relevance to the development of nanotechnology. Their specific behavior to external constraints, like temperature, electric field, magnetic field and radiations finds applications in many devices [**3**]. Cadmium Sulphide is a II-VI semiconductor with a direct band gap of 2.4 eV and has attracted much more attention because of its many potential applications in light detection such as in optical switches and filters. Due to its fluorescence property it can be also used as molecular probe in the diagnosis of cancer [**4**]. Photoswitchable magnetic nanoparticles containing CdS and Prussian blue created by Taguchi et al. **[5**] may open many possibilities in the development of magneto-optical devices. CdS doped with different transition metals which could work as multifunctional nanoparticles are being investigated for biomedical applications [**6**]. A novel strategy of designing composite nanoparticles (Gd_2O_3:Eu^{3+}) was developed by Tiwari et al. **[7]** in a similar way where spin-valve and other

magneto resistive devices detect the stray field from a magnetic nanobead. More recently, it has been reported that doping with transition metals in inorganic quantum particles like CdS could efficiently work as multifunctional nanoparticles **[8-9].** These functionalized nanoparticles are the futuristic materials for variety of applications starting from data storage, security/sensors to biomedical applications.

Most of the DMS nanoparticles can be synthesized by a variety of methods and can be made by substituting cations in compound semiconductors with transition metal ions [**10**]. Normally, chemical co-precipitation technique is relatively less expensive and convenient to prepare large area semiconductors. At moderate temperatures materials can easily be obtained in the colloidal form, which can subsequently be precipitated to give dry and stable powders. However, recently various suitable capping agents are being added in the reaction media to generate stabilized nanoparticles **[11].** In the present study chemical co-precipitation method has been adopted to prepare CdS:Mn samples in nano-crystalline form. Thiophenol was used as a capping agent to passivate the particles. Chemical composition, morphology, optical absorption and electrical conductivities of the samples were also investigated. In nano-crystalline materials both grains and grain boundaries play a vital role in modifying the electrical properties and have not been studied in detail with respect to their variation with dopant composition. In view of this, the present author has chosen to synthesize and characterize Mn doped CdS in nano-form by varying dopant concentration from 0 to 10 at.% and the results of all these studies are reported in this paper with relevant discussions.

Experimental

Chemicals

Cadmium acetate [$Cd(CH_3COO)_2$], Sodium sulphide nanohydrate ($Na_2S.9H_2O$) procured from Aldrich Chemical Co. Ltd., and Manganese acetate [$Mn(CH_3COO)_2$] purchased from Fisher Scientific Co. Ltd., were used as starting materials in this study. Mn doped CdS powders were synthesized according to the reported method **[12**] in our laboratory. All solvents and reagents obtained from commercial source were of analytical reagent (AR) grade and used as received.

Synthesis of nanosized CdS: Mn powder

CdS:Mn nanoparticles were prepared by colloidal chemical co-precipitation method. The chemicals used in the preparation were of analytical grade and were used without further purification. 0.1 M of Cd-acetate, 0.1 M of Mn-acetate and 0.1 M of sodium sulphide were prepared separately using methanol and distilled water as solvents. The solutions prepared from the starting materials in their respective solvents were taken in a round-bottomed flask fitted with a reflex-cooling tube. The contents were heated by a heating mantle, the vapours rise in the inner tube of the reflex, while the cooling water from a chilled is circulated in the outer jacket reflect the vapours back to the flask by condensing them. Hence, the quantity taken in the flask is invariable even after heating for hours together. The as-prepared solutions of Cd-acetate and Mn-acetate were mixed in the desired ratio and were taken in a burette. Solution of sodium sulphide and few drops of thiophenol were taken in a conical flask and were heated to 50 ^oC with magnetic stirring. Then the solution in the burette was added to a conical flask drop-wise at a run rate of 1ml/minute till turbidity (precipitation) occurred. The process involved the reaction of Mn^{2+} and Cd^{2+} ions with S^{2-} ions in the stoichiometric solution. Samples were prepared by varying the volume of Mn precursor keeping volumes of Cd acetate and sodium sulphide constant. In the solution CdS:Mn was precipitated which was washed several times with distilled water (peptization) to remove the byproduct Na-acetate salt. Then the samples were allowed to dry in a furnace at 300^0 C for 2h. Finally the dried powder of CdS:Mn was ground in an agate mortar and was characterized.

Characterization of nanosized CdS:Mn powder

The calcined samples were subjected to various characterization studies. The chemical species present in the samples were estimated using Energy Dispersive Analysis of X-rays (EDAX) attached to Scanning Electron Microscope (model: SEM, JSM 840A). For this purpose the powders were sprayed on a cylindrical metal rod and were capped with gold layer by sputtering method using ion sputtering device (model: JEOL JFC-1100E). By using the X-ray mode of SEM, the elements in the samples were identified.

The structural properties of the samples were investigated by powder X-ray diffractometer (XRD) (model: SIEFERT 3003 TT) with Cu K_α (λ=1.5420 Å) as target material using 40KV accelerating voltage, 30mA emission current and in the 2ɵ range of 20^0-80^0 with a scan rate of 1^0/min. The x-ray spectra were obtained by using a powder pattern indexing programme (POWD). This software has the capability of least square fitting and other routine refinements and directly outputs the lattice parameters data.

The fine structure of the powdered samples was analyzed by High Resolution Transmission Electron Microscope (HRTEM) (model: JOEL JEM 3010). Samples were prepared by placing a drop of the ethanol suspension of the nanopowders on a carbon coated copper TEM grid, which was sonicated for about 2 minute before placing it. Electrons of wavelength 0.025 Å at 200KV are transmitted through the samples were diffracted giving rise to structural information and unscattered electron beam produces bright field image of the samples.

FT-IR spectrum was recorded on FT-IR Spectrometer (model: MIR 8300™). The powders were mixed well with KBr and then palletized. The output spectrum was obtained by subtracting the background due to the solvent.

The absorption spectra of the samples were recorded on Cary-5E UV-VIS-NIR Spectrophotometer at room temperature in the range of 200-800 nm. The samples were diluted with nujol oil and ground well in a mortar. The resulting paste was then soaked on a whatmann-41 filter paper and was introduced into the spectrometer. Prior to that background correction was done with nujol-soaked filter paper. The impedance measurements were carried out on an Impedance Analyzer (model: Solartron SI 1260) with

a frequency range 0.1μ Hz to 32 MHz and fully automated with a personal computer which is controlled by software such as Z-plot/Z-view. This software directly outputs the bulk resistance, capacitance of the samples. Samples were made into pellets of thickness of 1mm and diameter of 8mm using hydraulic pressing with 1.75 Mpa before analysis in order to compute electrical conductivities of the samples.

Results and discussion

Mn doped CdS is distinguishable from other DMS, because of the half-filled 3d shell Mn can contribute its $4s^2$ electrons to the sp^3 hybridization in CdS and can substitutionally replace Cd atoms in CdS by forming a solid solution and allowing the possibility of tailoring its parameters like lattice constant, crystal structure, energy gap etc. To prepare the CdS:Mn nanoparticles through a simple method is of importance for both the physical research and the applications in opto-electronics. For doping transition metals into compound semiconductors, chemical co-precipitation method is the most conventional method than other synthesis methods like thermal decomposition, micro emulsion, hydrothermal synthesis and sonochemical synthesis **[13]**. It is cost effective and surfactant or stabilizer can also be added in the reaction media to produce stable nanoparticles. Hence, using the method yellow colored CdS: Mn powders were obtained. Preliminary XRD study showed that the samples were amorphous. The samples were calcined in a vacuum furnace at 100 ^{0}C, 200 ^{0}C and 300 ^{0}C followed by XRD. The samples calcined at 300 ^{0}C were found to be nanocrystalline in nature and these were subjected to various characterization studies.

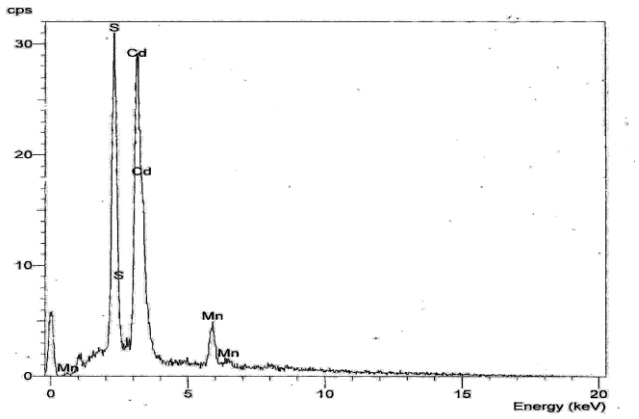

Fig. 1. EDAX pattern of Mn doped CdS sample.

Elemental analysis

Typical EDAX pattern of 10 atm. % Mn doped CdS is shown in **Fig. 1**. It can be seen that only peaks of cadmium (Cd), manganese (Mn) and sulfur(S) were detected, indicating the formation of CdMnS particles. The SEM micrograph of samples of the same Mn content is shown in **Fig. 2**. The micrograph shows spherical particles clustered together in aggregates. The agglomeration may occur due to the nanosize of the particles. The small nanocrystallites possess large surface energy, which leads the nanocrystallites to aggregate in order to lower their surface energy during formation of the nanocrystals [**14**].

.

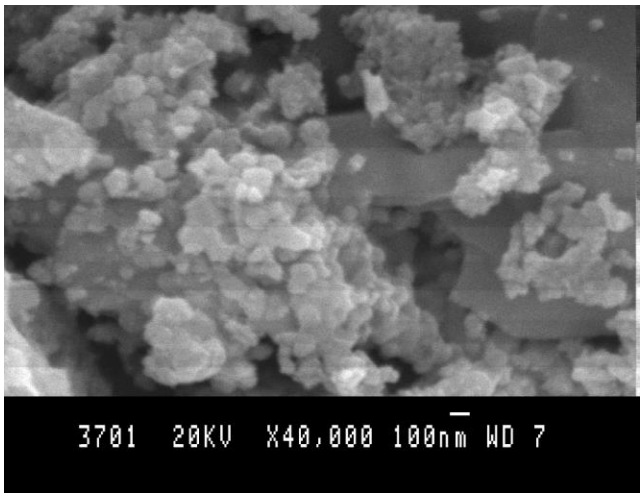

Fig. 2. SEM micrograph of Mn doped CdS sample.

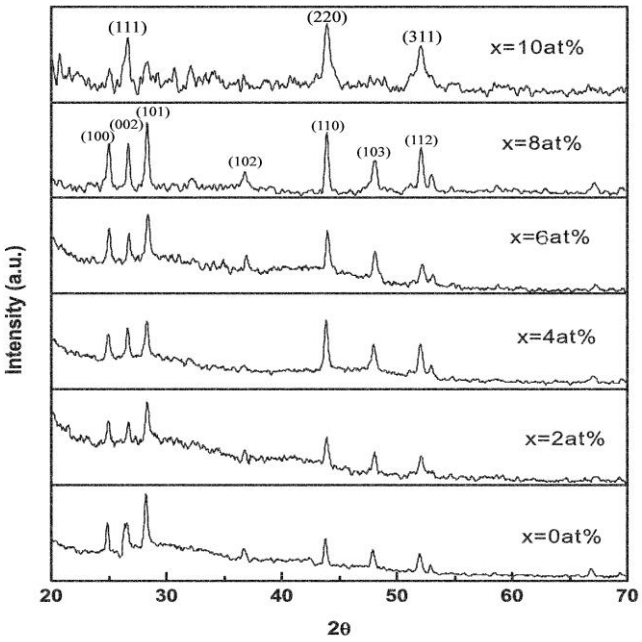

Fig. 3. X-ray diffraction scans of CdS: Mn samples.

Micro structural study

Fig. 3. shows the XRD patterns of all the Mn doped CdS samples. The X-ray lines are labeled with their respective crystallographic plane indices (hkl). An obvious change in the structure of the samples is observed with increase in 'Mn' content. The indexed peaks in the XRD patterns correspond to the hexagonal phase of CdS up to 8 at. % of Mn doping (JCPDS card 65-3414). But, on substitution of 10 at.% Mn the structure becomes cubic with lattice constant a =5.798 Å (JCPDS card 65-2887) indicating an obvious structural transformation. The grain size and the lattice parameters of the samples of all the compositions were calculated using XRD data and are shown in **Table 1**. The hexagonal phase lattice parameters 'a' and 'c' decrease

more or less linearly with increasing Mn content following Vegard's law [**15**]. This indicates that Mn has gone into the host lattice as a substituent, that is, 'Mn' ions occupy 'Cd' sites in the host CdS lattice. The crystallite size estimated from the full-width at half maximum (FWHM) intensity of the (110) and (220) reflections by using the Scherrer relation [**16**] varies in the range 13-30 nm for the samples of different Mn contents and is also shown in **Table 1**.

Table 1. XRD data of CdS: Mn nanoparticles.

Mn' content (at.%)	Angle (2θ)	Peak Width 2θ units	d-value (Å)	[hk1] (From XRD std.)	A (Å)	C (Å)	Crystallite size (nm)
0	43.7669	0.3030	2.0667	[110]	4.128	6.707	29
2	43.8264	0.3385	2.0640	[110]	4.123	6.697	26
4	43.8674	0.3818	2.0622	[110]	4.120	6.688	23
6	43.9043	0.3019	2.0605	[110]	4.117	6.676	30
8	43.9512	0.3806	2.0585	[110]	4.111	6.670	24
10	43.9756	0.6801	2.0574	[220]	5.798	--------	13

High- resolution TEM images of 10 atm. % Mn doped CdS are shown in **Fig. 4**. The ring pattern of the composite shown in **Fig. 4a**, confirms that the dispersed phase is cubic CdS, in consistence with the XRD observation. Examination of the particles at higher magnification known as lattice imaging (**Fig. 4b**) indicates that each of these large particles is polycrystalline and is an agglomeration of smaller particles with nanostructured domains. The tendency of the nanoparticles to agglomerate happens due to the lowering of free energy associated with the surface energy on forming larger particles **[17]**. The HRTEM image (**Fig. 4c**) shows quasi-spherical particles having sizes in 15-50 nm range. The size determined from XRD is always found to be smaller than that measured by HRTEM, since; XRD measures the crystallite size instead of particle size **[18]**.

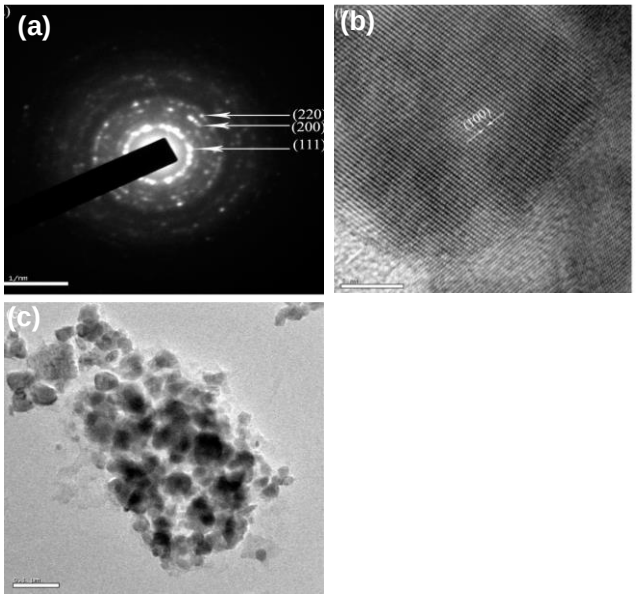

Fig. 4. HRTEM images of 10 at.% Mn doped CdS.

Optical study

Typical FT-IR spectrum of Mn doped CdS (10 atm. %) is shown in **Fig. 5**. In the higher energy region the peak at 3410 cm^{-1} is assigned to O-H stretching of absorbed water on the surface of the particles. Again, presence of water is confirmed by its bending vibration at 1627 cm^{-1}. The peak at 1436 cm^{-1} is attributed to bending vibration of methanol used in the process. It is also verified by its CH_3-stretching vibrations occurring as very weak peaks just below 3000 cm^{-1}. The C-O stretching vibration of absorbed methanol gives its intense peak at 1116 cm^{-1}. In addition to surface coverage of the samples by methanol, presence of thiophenol is also evident from this spectrum. Its ring C-H vibration occurs at about 3000 cm^{-1}, it is very weak peak. Similar such weak peaks due to C-H bending vibrations are observed at about 617 cm^{-1}. Hence, it can be inferred that the capping agent passivates the surface of the nanoparticles.

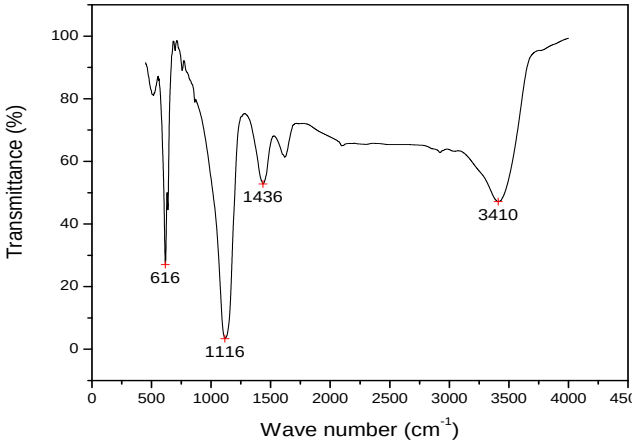

Fig. 5. FT-IR spectrum of 10 at% Mn doped CdS.

Optical absorption studies of the samples were carried out in the wavelength range of 200-800 nm at room temperature. The variation of absorbance with wavelength for CdS: Mn samples of all compositions is shown in Fig.6. The shape of the peaks for all Mn concentrations is similar and broad suggesting larger particle size distribution in consistence with the TEM results and also indicates that the nanoparticles are well quantum confined. Their absorption edge lies below 350 nm (3.54 eV), which is blue shifted from the bulk band gap value of CdS at 517 nm (2.40 eV) **[19]**. Blue shift is indicative of increasing band gap due to quantum size effect **[20, 21]** characteristic of nanosized particles. It is also observed that the optical band gap is found to vary nonlinearly with Mn content in CdS. Similar non-linear increase in the band gap of mixed $Cd_{1-x}Mn_xS$ nanocrystals with Mn content has also been reported earlier **[22]**. Whereas, Eychmuller et al. **[23]** reported that the increase in band gap energy could be attributed to decrease in particle size. This nonlinear dependence of the band gap on doping concentration is ascribed to band bowing which is believed to arise due to chemical disorder and exchange interaction between the band carrier and the d-electron of the magnetic Mn ion as suggested by Zunger et al. **[24]**. Chuu et al. **[25]** attributed the observed bowing in $Cd_{1-x}Mn_xS$ to inter substitutional atoms rather than to the

structure of the lattice itself. Besides, a slow decrease and increase in absorption is observed in the wavelength range of 350 nm to 200 nm. This corresponds to transitions to different excited states of the conduction band as described by Ekimov et al. **[26]**. Existence of surface states within the band gap region of the samples was also confirmed by photoluminescence study and will be published elsewhere **[27]**.

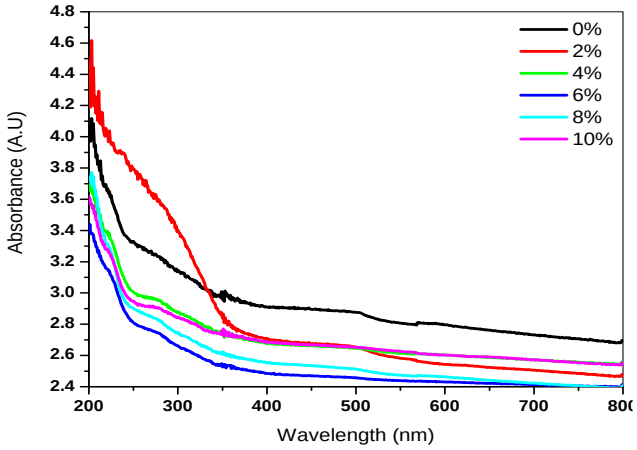

Fig. 6. UV-visible absorption spectra of CdS:Mn samples.

Electrical study

Fig. 7. shows the Cole- Cole plots (Nyquist plots) of the pelleted samples with different Mn content. Shielded test leads were used for electrical connections from the analyzer to the sample in order to avoid any parasitic impedance. All the semicircles exhibited some depression instead of semicircles centered on the x-axis. Such behavior is indicative of non-Debye type of relaxation and it also manifests that there is a distribution of relaxation time instead of a single relaxation time in the materials **[28]**. In addition to a semicircle, there exists a straight line at low frequencies in all the spectra, which is a characteristic of a double layer capacitance, that is, the capacitive admittance associated with the nanoparticles.

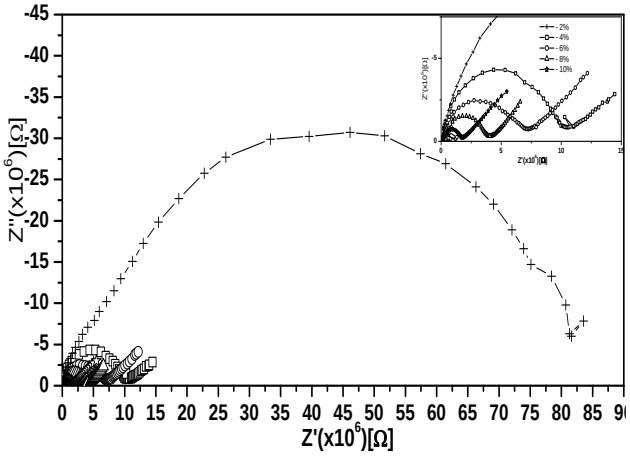

Fig. 7. Impedance plots of CdS: Mn samples and inset is hyperfine part of the doped samples.

Fig. 8. represents the two parallel RC circuits corresponding to grain and grain boundary effects, the proposed model for the impedance behavior shown in **Fig. 7**, where C_g is the bulk capacitance, R_g the bulk resistance, C_{gb} the grain boundary capacitance and R_{gb} the grain boundary resistance. The semicircles are attributed to bulk effect (intra granual) and the linear region is ascribed to grain boundary effect (inter granual) **[29]**. The grain boundaries may act as a hindrance to the carrier transport or they might also provide a high conductivity path (since the defect density may be larger in the interface region). Usually, a polycrystalline material shows both grain and grain boundary effects with different time constants leading to two successive semicircles **[30]**. The values of bulk resistance have been evaluated from the intercepts of semicircular arc on the real axis (z^1) and the d.c (bulk) conductivities of the samples were computed from known geometry of the pelleted samples and are shown in **Table. 2**. The resistivities of these samples are strongly dependent on Mn content and are of the order of a few MΩ-cm which are very much higher than that of the bulk CdS (0.12 Ω-cm at room temperature). The electrical resistivity of the nanocrystalline materials is expected to be higher than that of coarse grained poly crystalline materials, because of the increased volume fraction of atoms lying in the grain boundaries **[31]**. Similar high resistivity values for Mn doped ZnS nanoparticles were reported **[32]**. Further, this dielectric (insulating) nature of the samples is also anticipated due to the presence of large band gap in the samples. The resistivities of the samples decrease with increasing Mn content appreciably, this could be understood from the electronic structure of the component elements of the ternary alloy. According to Croce et al. **[33]** addition of Mn provides cross-linking centers for the CdS matrix lowers the tendency for sample reorganization and promotes a modification of the overall structure. Such a structural modification enhances the mechanical properties and establishes additional pathways for charge carriers to conduct at the surface of the samples.

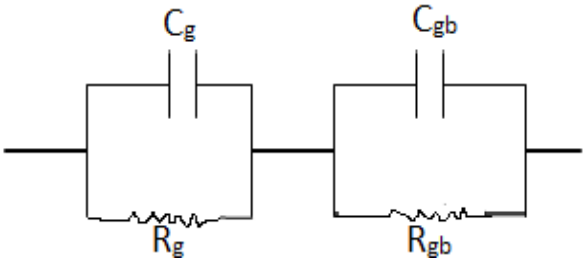

Fig. 8. The two parallel RC circuits equal to grain and grain boundary.

Table. 2. Bulk resistances and d.c conductivities of CdS: Mn samples.

'Mn' content (at. %)	**Bulk resistance** (ohm) x 10^6	**d.c. conductivity** (mho/cm) x 10^{-6}
2	85.49	0.009
4	10.53	0.075
6	7.71	0.103
8	3.98	0.200
10	1.88	0.416

CdS:Mn nano-polycrystalline particles were prepared at various Mn content (0-10 atm. %) by simple chemical co-precipitation method successfully using thiophenol as a capping agent. The composition of the samples is found to be CdMnS. XRD studies of the samples revealed structural transformation from hexagonal to cubic between 8 at.% and 10 atm. % of Mn doping and the crystallite size estimated from the broadening analysis generally corresponded to the primary particle size(grain size) as determined by HRTEM studies. Optical measurements showed a blue shift in the band gap energy of the samples and band bowing due to particles of varying sizes. Electrical studies indicated the insulating nature of the samples consistent with large band gap present in the samples and the doping of Mn on CdS enhances the electrical conductivities. The future challenge lies in designing monodisperse and nonagglomerated CdS:Mn nanoparticles that could bring us new opportunities to explore their properties and novel applications.

Reference

1. Furdyna, J.K. *J. Appl. Phys.* **1988,** *R29*, 64. **DOI:** 10.1063/1.341700.
2. Stankiewicz, J; Aray, A. *J. Appl. Phys.* **1982,** *53*, 3117. DOI: 10.1063/1.331007.
3. Tiwari, A.; Jin, C.; Kvit, A.; Kumar, D.; Muth, J.F.; Narayan, J. *Solid State Communi.* **2002,** *121*, 371. **DOI:** 10.1016/S0038-1098(01)00464-1.
4. Klimov, V.I.; Milkhailovsky, A.A.; Xu, S.; Malko, A.; Hollingsworth, J.A.; Leatherdale, C.A.; Eisler, H.J.; Bawendi, M.G. *Science*.**2000,** *290*, 314. **DOI:** 10.1126/Science.290.5490.314.
5. Taguchi, M.; Yagi, I.; Nakagawa, M.; Iyoda, T.; Einaga, Y. *J. Am. Chem. Soc.* **2006,** *128*, 10978. **DOI:** 10.1021/ja063461e.
6. Sharma, P. K.; Dutta, R. K.; Panday, A.C. *Adv. Mat. Lett.* **2011,** *2(4)*, 285. **DOI:** 10.5185/amlett.Indias.195.
7. Tiwari, A. *et al*, *Anal. Methods*, **2011**, 3, 217. **DOI:** 10.1039/C0ay00574f.
8. Tiwari, A. Biomedical Materials and Diagnostic Devices, wiley-Scrivener Publishing, LLC, USA, ISBN 978-11-180301-41, **2012.** **DOI:** 10.1002/9781118523025.
9. Sharma, P.K.; Dutta, R.K.; Pandey, A.C. *Adv.Mat.Lett.***2011**, *2(4)*, 246. **DOI:** 10.5185/amlett.2011.indias214.
10. Ohno, H. *Science* **1998,** *281*, 951. **DOI:** 10.1126/Science.281.5379.951.
11. Tiwari, A.; Mishra, A.K.; Kobayashi, H.; Turner, A.P.F. *Intelligent nanomaterials*, Wiley-scrivener Publishing, USA, ISBN 978-04-709387-99, **2012.** **DOI:** 10.1002/9781118311974.
12. Veinot, J.G.C.; Ginzburg, M.; Pietro, W.J. *Chem. Mater.* **1997,** *9*, 2117. **DOI:** 10.1021/cm970189m.
13. Jadhav, S.A.; Bongiovanni, R. *Adv.Mat. Lett.* **2012,** *3(5)*, 357. **DOI:** 10.5185/amlett.2012.7381.
14. Srivastava, N.; Srivastava, P.C. *Bull. Mater. Sci.* **2010,** *33*, 654. **DOI:** 10.1007/S12034-011-0142-0.
15. Yoder-short, D. R.; Debska, U.; Furdyna, J. K. *J. Appl. Phys*. **1985**, *58*, 4056. **DOI:** 10.1063/1.335585.
16. Sun, J.; Zhou, S.; Hou, P.; Yang, Y.; Weng, J.; Li, X.; Li, M. *J. Biomed. Mater. Res. Part A.* **2007,** *80A,* 323. **DOI:** 10.1002/jbm.a.30909.
17. Sun, W. et al. *Chem. Mater***. 2007**, *19*, 1772. **DOI:** 10.1021/cm061741n.
18. Yuang, Y.S.; Chem, F.Y.; Leeiu, Y.Y. *Jpn. J. Appl.* **1994,** *76*, 3041. **DOI:** 10.1063/1.357483.
19. Shen, G.Z.; Cho, J.H.; Yoo, J.K.; Yi, G.C.; Lee, C.J. *J. Phys. Chem.* **2005,** *B109*, 9294. **DOI:** 10.1021/jp044888f.
20. Henglein, A. *Chem. Rev.* **1989,** *89*, 1861. **DOI:** 10.1021/cr00098a010.
21. Valenta, J.; Dian, J.; Gillot, P.; Hanerlage, B. *Phys. Status. Solidi.* **2001,** *13224*, 313. **DOI:** 10.1002/1521-3951(200103).
22. Levy, L.; Ingert, D.; Feltin, N.; Pileni, M.P. *J. Cryst. Growth*, **1998**, *184-185*, 377. **DOI:** 10.1016/S0022-0248(98)80080-8.
23. Eychmuller, A.; Hasserlbarth, A.; Katsikas, L.; Weller, H.; Ber. Eunseges. *Phys.Chem.* **1991**, *95*, 79. **DOI:** 10.1021/j100154a019.
24. Zunger, A.; Jaffe, J.E. *Phys. Rev. Lett.* **1983,** *51*, 662. **DOI:** 10.1103/PhysRevLett.51.662.
25. Chuu, D. S.; Chang, Y.C.; Hsieh, C. Y. *Thin Solid Films.* **1997**, *304*, 28. **DOI:** 10.1016/S0040-6090(97)00142-9.
26. Ekimov, A.I. et al. *J. Lumin.* **1990,** *46*, 83. **DOI:** 10.1016/0022-2313(90)90010-9.
27. Venkatesu, P.; Ravichandran, K. *Adv. Mat. Lett.* **2013,** *4(3),* 202. **DOI:** 10.5185/amlett.2012.7379.
28. Song, J.Y.; Lee, H.H.; Wang, Y.Y.; Wan, C.C. *J. Power Sources.* **2002,** *111*, 255. **DOI:** 10.1016/S0378-7753(02)00310-5.
29. Rahmouni, H.; Nouiri, M.; Jemai, R.; Kallal, N.; Rzigua, F.; Selmi, A.; Khirouni, K.; Alaya, S. *J. Magn. Magn. Mater.* **2007,** *316*, 23. **DOI:** 10.1016/j.jmmm.2007.03.208.
30. Behera, B.; Nagak, P.; Choudhary, R.N.P. *J. Alloys. Compd.* **2007,** *436*, 226. **DOI:** 10.1016/j.jallcom.2006.07.028.
31. Wang, Y.Z.; Qiao, G.W.; Liv, X.D.; Ding, B.Z.; Hu, Z.Q. *Mater. Lett.* **1993,** *17*, 152. **DOI:** 10.1016/0167-577X(93)90075-9.
32. Karar, N.; Suchitra Raj.; Singh, F. *J. Cryst. Growth.* **2004,** *268*, 585. **DOI:** 10.1016/j.jcrysgro.2004.04.096.
33. Croce, F; Persi, L; Scrosati, B; Serraino-Fiory, F; Plichta, E; Hendrickson, M.A. *Electrochim. Acta*. **2001**, *46*, 2457. **DOI:** 10.1016/S0013-4686(01)00458-3.